

## Fluid mixing and particle suspension in a novel microreactor

A. Harvey<sup>1</sup>, M.R. Mackley<sup>1</sup>, N. Reis<sup>2,\*</sup>, J.A. Teixeira<sup>2</sup>, A. A. Vicente<sup>2</sup>

<sup>1</sup>Department of Chemical Engineering, University of Cambridge, New Museum Site, Pembroke Street, CB2 3RA Cambridge, UK. Phone: +44.(0)1223.334777; Fax: +44.(0)1223.334796

<sup>2</sup>Centro de Engenharia Biológica, Universidade do Minho, Campus de Gualtar, 4710-057 Braga, Portugal. Phone: +351.253.604400; Fax: +351.253.678986

**Keywords:** continuous microreactor, CFD, PIV, oscillatory flow, heterogeneous catalysis

### 1. Introduction

On catalysis and reaction engineering, new reactor designs at a micro scale are desirable, which could guarantee a scale-down of the production of high valuable products, decreasing the reagents needs and the industrial unit space requirements. Thus, a new reactor design should guarantee a good fluid mixing for applications on the manufacture of specialty chemicals but also be able to keep particles suspended, with a high range of densities for several industrial purposes such as combinatorial (homogenous or heterogeneous) and high-throughput screening catalysis.

Furthermore, sequential reactions are of frequent use in these kinds of industries and a single reactor volume able to perform different reactions would be very useful.

A novel continuous reactor composed of micro scaled tubes and based on oscillatory flow technology is presented as a new solution for those industrial applications.

Since the early 1990s, studies have shown that periodically spaced orifice baffles along the length of a tube, with a net flow coupled with a reversing oscillatory component of the correct magnitude, give high fluid mixing and narrow residence time distribution (Brunold *et al.*, 1989; Dickens *et al.*, 1989; Howes *et al.*, 1990; Mackley and Ni, 1991, 1993). The baffle edges promote the formation of eddies, which increase the radial mixing in the tube, leading to radial velocity values of the same order of magnitude as the axial velocities (e.g. Macklay, 1990; Mackley and Ni, 1991; Ni and Pereira, 2000).

The efficiency of the mechanism for moving fluid from the walls to the centre of the reactor is affected by many variables, such as the oscillation frequency ( $f$ ), amplitude ( $x_0$ ), reactor internal diameter ( $d$ ), baffle spacing ( $L$ ), baffle internal diameter ( $d_0$ ), baffle thickness ( $\delta$ ) and by the fluid rheological properties (density,  $\rho$ , and viscosity,  $\mu$ ) and net flow Reynolds number ( $Re_n$ ), when existing. The intensity of mixing applied to a OFR is described by the oscillatory Reynolds number,  $Re_o$ , which is defined as  $2\pi \cdot f \cdot x_0 \cdot \rho \cdot d \cdot \mu^{-1}$  (Ni *et al.*, 2000, 2002; Ni and Gough, 1997).

From extensive studies, it is known that at  $Re_o$  values of 100-300, the OFR exhibits a near plug flow behaviour, where the vortice rings are symmetrically generated within each baffle cavity. For values of  $Re_o$  above a critical value, the flow becomes intensely mixed and chaotic and the OFR behaves as a stirred tank (Ni *et al.*, 1999, 2002). In this case, the generation of vortices is no longer axisymmetrical (Ni *et al.*, 2002). These results are consistent for reactors with different diameters (at 25 and 50 mm), indicating that the fluid mechanical conditions in a OFR can be linearly scaled up (Brunold *et al.*, 1989; Dickens *et al.*, 1989; Ni *et al.*, 1995b). However, fluid mechanics at micro scales (in the range of millimeters) have not been studied previously.

Flow visualization experiments reported by Ni *et al.* (1995a) shown that fluid oscillation in an OFR is an efficient way of keeping particles in suspension and well-mixed. Also the OFR has proved to be a good particle separator as reported by Mackley *et al.* (1993).

The fluid mechanics of the novel oscillatory flow micro reactor (micro-OFR) was studied and the experimental conditions in which the new micro reactor is able to keep different particles suspended were investigated. Some design aspects relating to the novel micro reactor were evaluated and will be presented in this text, for the first time.

Also numerical simulations using the commercial software Fluent (Fluent Co., U.S.A.) were aiming at understanding the fluid mixing characteristics presented by the novel micro-OFR.

## 2. Materials and Methods

### 2.1 Micro reactor and experimental facilities

A 35 cm long and 4.4 mm internal diameter glass jacket tube (Fig. 1) has been hold up in a support that permits the 2-D rotation around a support point. This tube was composed of smooth periodic cavities (SPC), with an averaged baffle spacing of 13 mm (or 3.d) and a baffle thickness of 6 mm. The diameter on the constricted zone (baffle internal diameter) was 1.6 mm, leading to a baffle free area of 13 %.

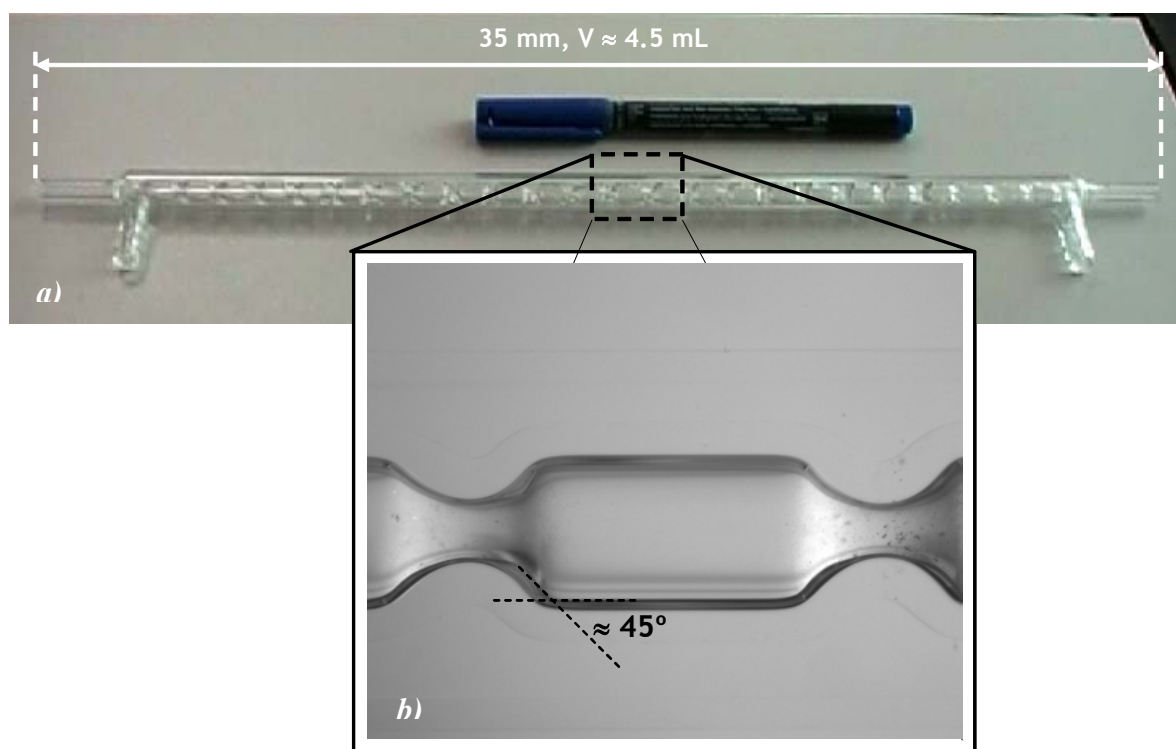


Fig. 1 Geometry of: (a) a tube element of the novel micro-OFR and (b) a smooth periodic cavity.

The fluid was oscillated using a piston device, moved by an electromagnetic oscillator. The piston oscillation frequency was controlled using a precise signal generator and the oscillation amplitude was controlled by power setting. Oscillation frequencies of 0 to 50 Hz and amplitudes of 0 to 20 mm centre-to-peak were possible, but due to the type of oscillator unit used, high oscillation amplitudes were only possible at low frequencies, and vice-versa.

All the experiments were performed on batch mode and all the amplitudes expressed as centre-to-peak.

### 2.2 Particle image velocimetry

At the beginning of each experiment, neutrally buoyancy silvered particles with a mean particle diameter of  $10 \mu\text{m}$  were used as tracer particles and pumped to the SPC to give a seeding to liquid ratio of  $10^{-5}:1$ , as recommended by Elgobashi (1994) as the optimal seeding density. For each run, the seeded fluid was oscillated for 5 min before image acquisition starts. All experiments were performed at room temperature (ca.  $20^\circ\text{C}$ ).

A quadrangular Perspex optical box was fitted around the centre of the SPC tube and filled with glycerol to minimize optical distortions (due to the circular geometry of the tube). Also the space between the internal and external SPC tube walls (jacket inter-space) was filled with glycerol. The light source was a Nd:Yag dual pulsed laser, with a wave length of 520 nm and a maximum power intensity of 30 mJ. The beam was turned into a vertical light sheet, 1mm thick, and calibrated to cross the middle of the flow field.

A low frequency digital camera was located perpendicularly to the laser source and parallel to the optical box. As the PIV system is limited to low image acquisition frequencies (1 to 4 Hz), a phase difference of 0.1 Hz was used between the camera capture and oscillator unit to obtain the velocity profiles at different piston positions. This allowed 10 equally spaced phase images per full cycle. The phase angle of a picture is determined from either reading the level meter captured at the same moment with a second digital camera, or by post-processing analysis of the axial average velocity profile of each experiment. It should be noted that phase angle could not be reproduced between different experiments.

The cameras were synchronised with the laser source by means of an ILA synchroniser, which allows controlling the camera exposure settings, namely the pulse distance (time distance between two consecutive laser pulses) of each experiment.

The velocity vector maps for each image-pair were produced by interrogating small bus-regions (known as interrogation areas). This practise determines the average displacement between images. The results were processed using VidPIV® software and then plotted using TECPLOT® software. Each experiment consisted of acquisition of 30 images for each experiment, permitting 3 equal phase images for each cycle position. Then, the instantaneous velocity vector maps were constructed for each image. The phase-averaged properties were obtained by averaging those 3 images of each individual phase in an oscillation cycle.

Experiments were carried out for many combinations of oscillation frequencies and amplitudes, resulting on fifteen amplitude-frequency combinations. This corresponds to  $Re_o$  values from 12 to 1335, covering both the expected axisymmetric and non-axisymmetric regimes for the SPC geometry (Mackley and Ni, 1991; Mackley, 1990; Howes et al., 1991; Mackley, 1991).

Initially, six experiments were carried out at constant oscillation amplitude of 1 mm, using oscillation frequencies at 4.1, 5.1, 10.1, 11.1, 15.1 and 20.1 Hz, leading to  $Re_o$  values of 117 to 630. Then, four more experiments were done at a constant oscillation frequency of 2.1 Hz (0.2, 0.3, 3 and 5 mm) and two more at a constant oscillation frequency of 1.1 Hz (4 and 11 mm). Finally, intending to test the possible effect of the gravity over the fluid mechanics and also over the particle suspension, two more series of experiments were done at two oscillation frequencies of 4.1 Hz and 12.1 Hz, for an oscillation amplitude between 3 and 4 mm, but at different angle positions of the SPC tube: 90° (vertical position), 45° and 10° degrees.

### *2.3 Computation fluid dynamics*

The CFD package used in this work is based on Fluent 5.5 (1998). The 3-D Navier-Stokes equations are solved directly, which guarantees a conservation of the momentum and continuity inside the simulated mesh.

The simulations started with 2-D continuous flow and then with unsteady laminar conditions. A planar and an axisymmetrical mesh were used to test the differences between these 2-D laminar submodels. Laminar 3-D numerical simulations and 3-D Large Eddy Simulations (LES) were subsequently used. Different cells spacing between 0.3 and 0.05 mm were used to test the mesh independency at steady and unsteady flow conditions.

Meshes were created using Gambit 1.2.2 software and according to the simulations settings and with a geometry, in all the cases, with the same dimensions as the SPC (Fig.1). Once the intention is to simulate the fluid mechanics inside a cavity in the centre of the tube, the velocity profiles in the inlet and outlet of a SPC should be the same. This is equivalent to say that a micro-OFR tube has a periodicity in terms of geometry and velocity profile and this can be imposed in Fluent by using periodic boundary conditions (periodic BC's).

The numerical simulations procedures involved solving the governing equations sequentially using the segregated method solver. Under-relaxation was used to control the change of scalar variables in every iteration. In terms of discretisation schemes, the pressure was a second-order scheme, the momentum and turbulent parameters were a second-order upwind schemes. The SIMPLEC algorithm was employed in the pressure-velocity coupling scheme.

#### *2.4 Particles and bubbles suspension*

To test the performance of the micro-OFR on suspension of particles, some particles were injected through the top of the tube and oscillated until a steady concentration distribution was achieved. Three different kinds of particles used in catalysis field were tested, namely, *a)* silica resin, *b)* polyamine resin and *c)* ionic exchange resin. Maximum sedimentation velocities were determined by measuring the distance and time travelled by a particle in a 500 mL provette, filled with water. Five assays were done for each type of particles and the average achieved value for particles *a)* to *c)* was, respectively, 23, 1.5 and 2.5 mm.s<sup>-1</sup>. It should be noted that particles *b)* also present some negative buoyancy particles, which is very interesting in order to test the capacity of the micro-OFR to keep negative buoyancy particles suspended.

A small mesh, made of polyethylene fibre, was fitted to the bottom of the tube to avoid particle sedimentation and entrance into the piston when the oscillation was stopped.

Different particle concentrations were used.

For bubbles suspension experiments, a few bubbles were injected in the bottom of the tube while the oscillation conditions were kept constant. All the experiments were recorded at the centre of the tube, through the optical box, using a digital Samsung handy camera at 25 frames per second, illuminated at the top by a 50W lamp.

### **3. Results and discussion**

#### *3.1 Fluid mechanics study by PIV*

The first task of the experimental work concerned with the study of fluid mechanics of the micro-OFR at different oscillation conditions. This was made only for the batch mode, since it represents the worst hydrodynamic conditions for particle suspension applications. Furthermore, it has been previously showed that a small net flow does not affect significantly the oscillatory patterns (Stonestreet and Harvey, 2002).

The PIV consisted on the acquisition of thirty (dual) images for each experiment. Then, the instantaneous velocity vector maps were built as well as the phase-averaged velocity vector maps for each of the ten angle phases, by averaging three velocity vector maps. More than 500 velocity vector maps were performed and just a few of them will be presented here. Only the phase-averaged velocity maps are presented in this text as, during inspection of the sequence of images, it was noted that the characteristics of the phase-averaged velocity vectors were generally similar to those of the instantaneous velocity maps, but with a much more evident axisymmetric nature.

In Fig.2, three phase-averaged velocity vector maps are presented, at 1/5<sup>th</sup> of an oscillation cycle (piston reaching the maximum stroke position, just before flow reversing, i.e. velocity decreasing and reaching a null value). This point was selected since it was found that it coincides mostly with the maximum shear strain rate and the eddy activity is more detectable.

Symmetrical eddy structures were detectable at a  $Re_0$  of 12 (Fig. 2a) and this can be specified as the critical  $Re_0$  of transition between the laminar flow regime and the conditions leading to the appearance of the first axisymmetric eddies. The increase of oscillation mixing intensity brakes axisymmetry of toroidal rings at  $Re_0$  values of about 100, leading to high axial mixing and the micro-OFR behaves as a stirred tank. In Fig. 2b it is clearly detectable the non-axisymmetry of eddies at 1/5<sup>th</sup> of an oscillation cycle and at a  $Re_0$  of 203. Minimal critical oscillatory Reynolds numbers found for micro-OFR are summarised in Table 1.

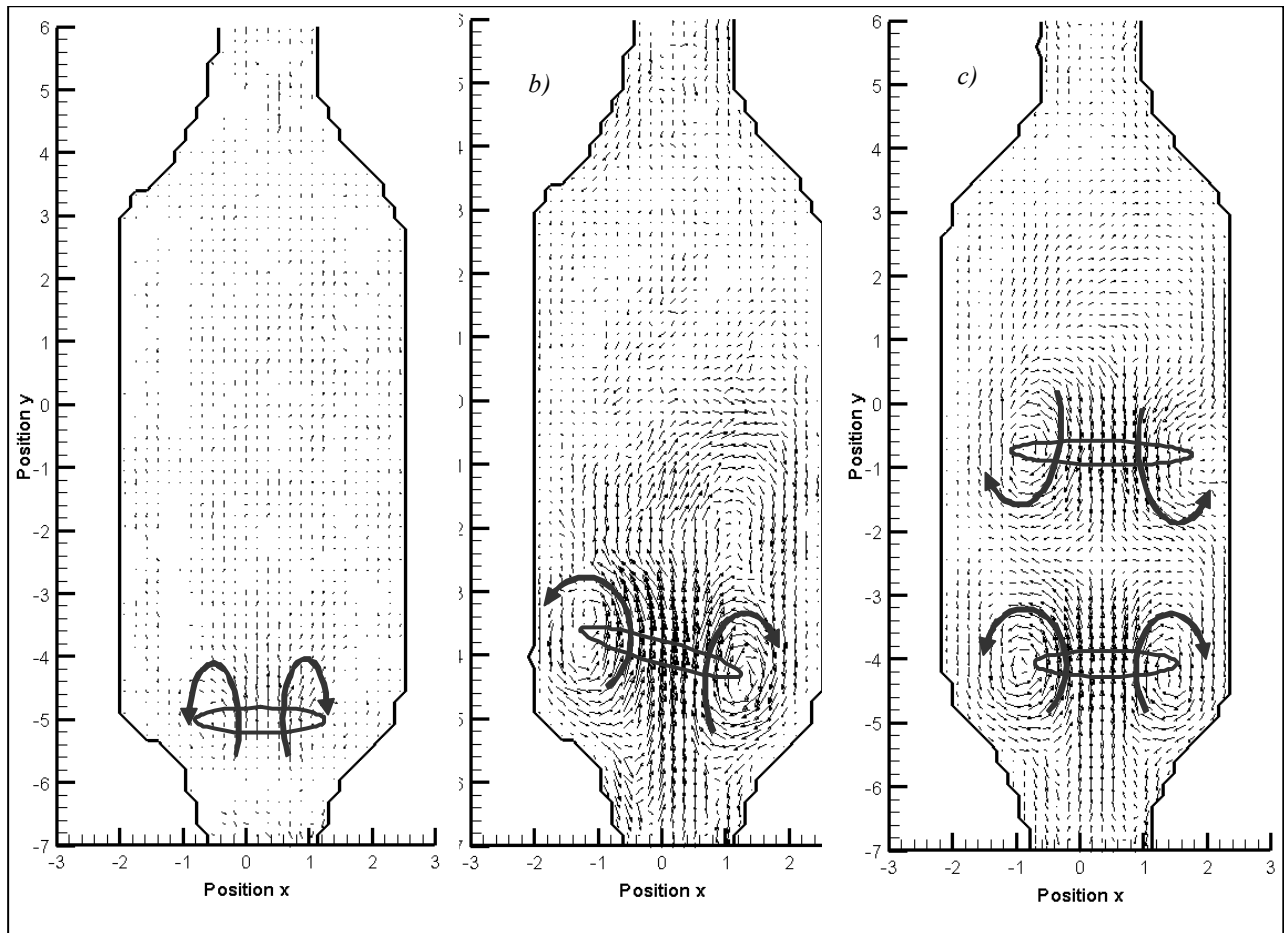


Fig.2 Phase-averaged velocity vector maps at  $1/5^{\text{th}}$  of an oscillation cycle for different oscillation conditions: (a)  $Re_o = 12$ ,  $x_0 = 0.2$  mm,  $f = 2.1$  Hz; (b)  $Re_o = 203$ ,  $x_0 = 1.4$  mm,  $f = 5.1$  Hz; (c)  $Re_o = 348$ ,  $x_0 = 1.1$  mm,  $f = 11.1$  Hz.

Table 1 Critical  $Re_o$  for the micro-OFR and comparison with some reported values for the conventional OFR

Toroidal rings geometry	Reactor mixing conditions	micro-OFR	conventional OFR	
Axisymmetrical	Low axial mixing (or near plug flow behaviour at continuous flow)	$Re_o > 10$	$Re_o > 50$	Mackley and Ni, 1991
			$Re_o > 75$	Mackley, 1990
Non-axisymmetrical	Stirred tank behaviour	$Re_o > 100$	$Re_o > 300$	Howes et al., 1991
			$Re_o > 400$	Mackley, 1991

The effect of amplitude was proved to be different from the effect of the oscillation frequency, as opposed to the reported in the conventional OFR studies (e.g., Ni and Pereira, 2000; Mackley and Ni, 1993). For instance, different fluid mechanics are achieved at similar  $Re_o$  of 117 and 116, but at oscillation conditions of 4.1 Hz/1.0 mm and 1.1 Hz/3.8 mm, respectively. In the first case, eddy structures are completely axisymmetrical but, in the second one, axisymmetry was clearly broken. Further experiments at high  $Re_o$  (above 200) but at low oscillation amplitudes ( $\leq 1$  mm) and at high oscillation frequencies ( $\geq 5.1$  Hz) present a smaller non-axisymmetry index when compared with experiments at high oscillation amplitudes and low frequencies. An example is presented in Fig. 2c, for a  $Re_o$  of 348, where eddies are non-axisymmetric.

It was also observed that the increase of oscillation frequency at small amplitudes (below 1 mm) tends to stabilise the flow, essentially for  $Re_o$  above 450: the number of detectable eddy structures on each velocity vector map increases with the increase of oscillation frequency as well as the intensity of each eddy structure. Consequently, toroidal rings become axi-symmetric in most of the phase angles except near flow reversing.

Further PIV experiments at different tube position angles showed that fluid mechanics is not affected by gravity and that for particle suspension very intensive eddy structures are required in all phase angles, which is guaranteed by operation at high oscillation frequencies. Even for a  $Re_o$  of

1335, performed at 12.1 Hz and 4 mm (found to be the optimal oscillation conditions for keeping particles suspended), the flow is not completely chaotic and very intensive eddy structures were detected throughout a full oscillation cycle.

### 3.2 CFD simulations

Numerical simulations using the software Fluent were made for a wide range of flow conditions. Firstly, 2-D laminar simulations were performed for continuous and oscillatory flow using a 2-D planar and a 2-D axisymmetric mesh. Mesh independency at 2-D was tested and it was found to exist for cells spacing of 0.1 mm, in the straight zone, and a non-uniform gradient of 0.05 to 0.075 mm, in the smooth constricted zone. This led to a planar mesh with 13,640 cells and an half of this number in the axisymmetric mesh.

Flow on the inverse direction was detected near the bottom baffle at a continuous net flow rate above 2.3 mm/s, corresponding to a net flow Reynolds number ( $Re_n$ ) of 10. The increase of the  $Re_n$  led to an increase of the flow in the inverse direction.

Simulated flow patterns using a 2-D laminar axisymmetric model showed a qualitative agreement with PIV measurements. For low axial mixing conditions ( $Re_o$  below 100), there is a complete agreement of PIV with the 2-D laminar axisymmetric CFD simulations in terms of location, number and size of vortices.

For  $Re_o$  above 100, the PIV clearly shown the existence of non-axisymmetric toroidal rings and, not surprisingly, 2-D axisymmetric model is not able to simulate this non-axisymmetry. However, flow patterns simulated at high  $Re_o$  but at low oscillation amplitudes (below 1 mm) present a semi-quantitative agreement with PIV results: unlike non-axisymmetry, the relative position of toroidal rings in the cavity as well as the number of visible eddy structures on each angle phase agrees with visualisations. An example is presented in Fig. 3a and carried out at a  $Re_o$  of 450 (20 Hz and 0.8 mm). Only the flow pattern in the central cavity is presented. The simulated flow patterns coincides with the measurement made by PIV at similar oscillation conditions ( $Re_o = 348$ ,  $x_0 = 1.1$  mm,  $f = 11.1$  Hz) and shown in Fig. 2c.

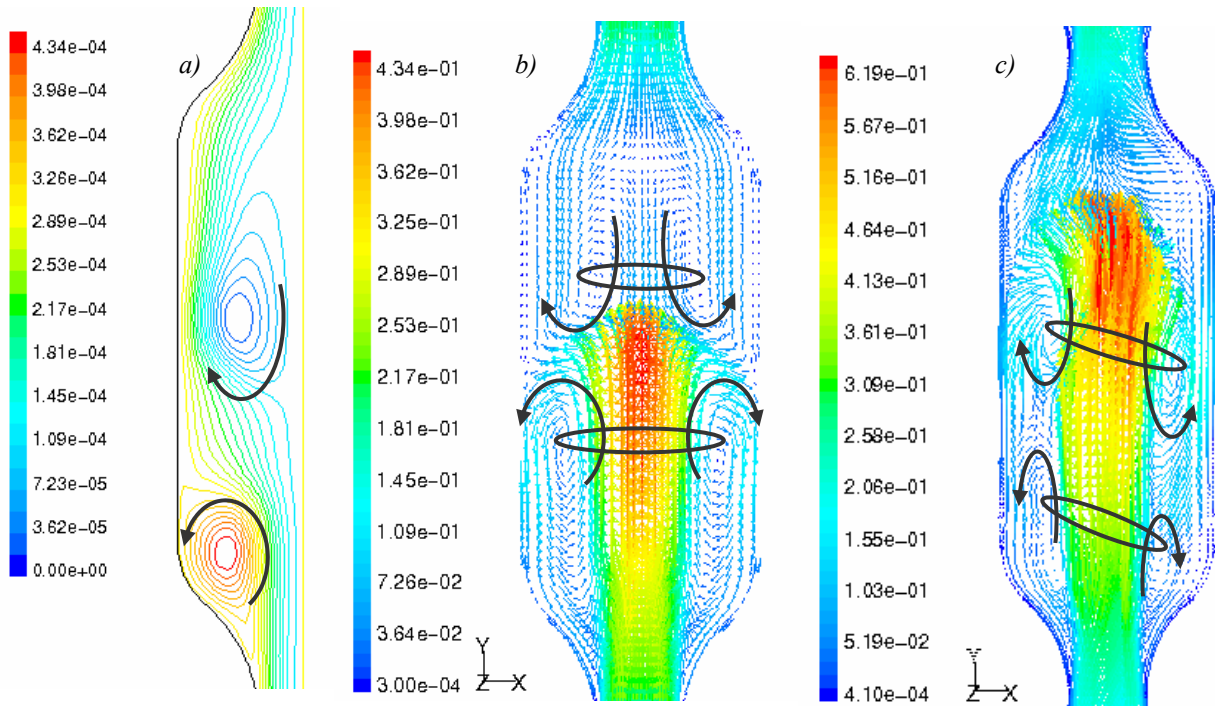


Fig.3 Flow patterns of CFD at 1/5<sup>th</sup> of an oscillation cycle using different solver models: (a) contours of stream functions (Kg/s) using 2-D laminar axisymmetric model,  $Re_o = 450$ ,  $f = 20$  Hz,  $x_0 = 0.8$  mm, 2<sup>nd</sup> simulated cycle; (b) velocity vectors coloured by velocity magnitude (m/s), on plane  $z = 0$ , using 3-D laminar model,  $Re_o = 350$ ,  $f = 10$  Hz,  $x_0 = 1$  mm, 9<sup>th</sup> simulated cycle; (c) velocity vectors coloured by velocity magnitude (m/s), on plane  $z = 0$ , using 3-D LES model,  $Re_o = 350$ ,  $f = 10$  Hz,  $x_0 = 1$  mm, 4<sup>th</sup> simulated cycle.

It was confirmed that oscillation frequency affects more significantly the flow than the oscillation amplitude: the use of small amplitudes leads to an increase of eddy intensity (smaller eddy size). On the contrary, the use of high oscillation amplitudes increases the eddy size and decreases the number of visible eddy structures at each phase angle.

Results from 2-D planar simulation were slightly different from the 2-D laminar axisymmetric simulations. From comparison with PIV velocity vector maps, it was concluded that results from the axisymmetric model are a better representation of the reality than the results from the planar simulations: the simulated size of eddy structures given by the planar model tend to be exaggerated and not so intensive as it should be by the PIV observations.

Unlike the simulations based on conventional geometry (Howes et al., 1991; Ni *et al.*, 2002), it was not possible to break axisymmetry using the 2-D planar laminar model, even for  $Re_0$  above 1000. This suggests a new effect of SPC geometry on the oscillatory flow. Consequently, 3-D simulations were needed to simulate non-axisymmetry.

In terms of 3-D, the decrease of mesh cell size compromises the viable computing simulation time, since the number of cells is incredibly increased (Fig. 4). So, a compromise was found between convergence due to the chosen mesh and results resolution. The selected cell spacing for 3-D laminar simulations was 0.2 mm, leading to a mesh with 68,544 cells. Since the LES model requires a finer mesh, essentially near the walls (to enable simulation of laminar layer), the number of cells near the wall was increased by means of a boundary layer, leading to a mesh with more than 78,000 cells.

The oscillation conditions used in 3-D simulations were the same as these on experiment c) in Fig. 2, e.g.  $Re_0 = 348$ ,  $x_0 = 1.1$  mm,  $f = 11.1$  Hz. In Fig. 3 b) and c), respectively, simulated flow patterns using laminar and LES model are presented.

The 3-D laminar model was unable to simulate non-axisymmetry. An example is presented in Fig. 3b. Apparently, it seems that the new SPC geometry stabilises the flow, when compared with the conventional OFR geometry for specific oscillation conditions. Anyway, it should be remembered that the critical Reynolds numbers detected by PIV are lower for SPC geometry than for conventional OFR geometry (Table 1), i.e. non-axisymmetry occurs early in the micro-OFR than in the OFR. It means that, in fact, more energy is dissipated than the energy that the laminar model is able to simulate. Contrary to the results obtained by Ni *et al.* (2002), who claims that the uniform mixing in an OFR is independent of turbulence intensity and is due to “laminar instabilities”, the laminar model is not able to simulate non-axisymmetry in the present case. A model able to simulate turbulence energy dissipation was needed and, consequently, LES model at 3-D was used to simulate the flow patterns at high  $Re_0$  (Fig. 3c). The flow patterns presented in Fig. 3c shows the velocity vector map at the same conditions as Fig. 3b but now using a 3-D LES model. This model is in fact suitable on predicting the non-axisymmetry inside the new SPC geometry.

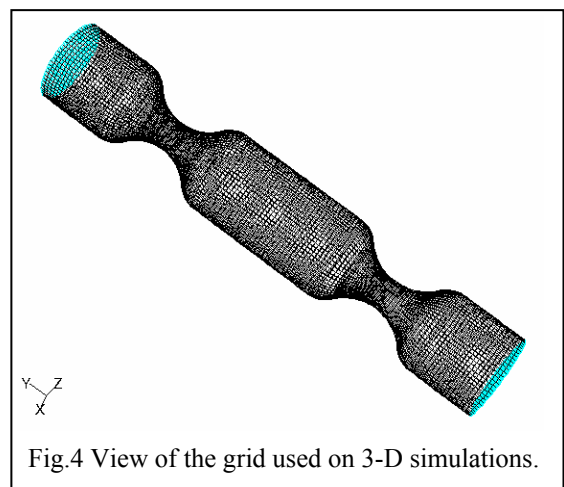


Fig.4 View of the grid used on 3-D simulations.

### 3.3 Visualisation of particles and bubbles suspension

#### 3.3.1 Effect of the concentration of particles

To test the performance of the micro-OFR on the suspension of particles, a wide range of experiments was done using three kinds of particles, at different combinations of oscillation frequency, oscillation amplitudes and particle concentrations.

In Fig. 5, the relation between the oscillation conditions and the maximum suspended concentration of silica particles is presented, with the tube at the vertical position, with no visible concentration profile between the top and the bottom of the tube. The maximum concentration of silica particles



(40 % v/v) in well mixed conditions was achieved at 12.1 Hz and 4 mm. Other oscillation conditions at similar  $Re_0$  were impossible to achieve due to the limitations of the maximum amplitude and frequency of the oscillator unit. Consequently, those were considered the better oscillation conditions for particle suspension applications. The oscillation frequency shows a different effect from that of the oscillation amplitude in terms of the particle suspension: it is easier to suspend particles at high frequencies and low amplitudes than at low frequencies and high amplitudes. This is coherent with the PIV results and proves that particle suspension inside the micro-OFR is correlated with the fluid mechanics.

At the same optimal oscillation conditions, the micro-OFR was able to keep 15 % (w/w) of polyamine particles completely suspended. It was observed that the micro-OFR is not only able to keep particles suspended but also to re-suspend sedimented particles in a few seconds.

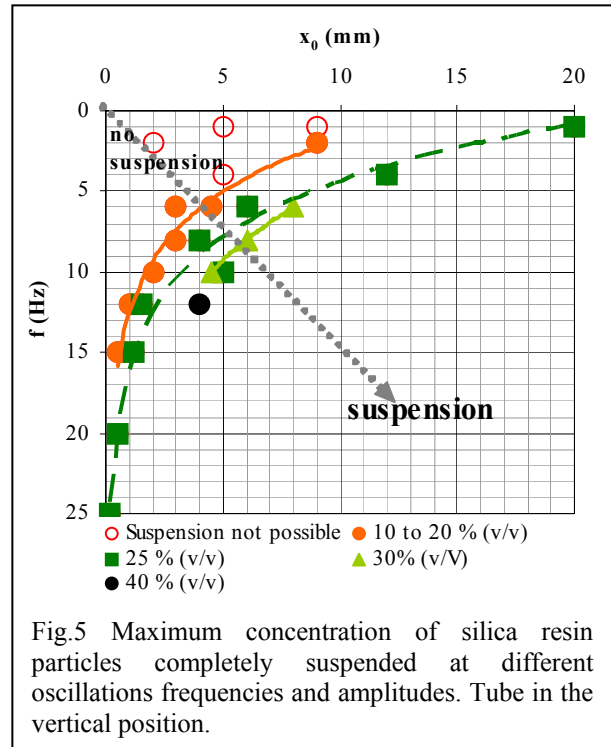


Fig.5 Maximum concentration of silica resin particles completely suspended at different oscillations frequencies and amplitudes. Tube in the vertical position.

### 3.3.2 Effect of the reactor angle over particles and bubbles suspension

The effect of the angle of the reactor on the particle suspension was also studied. In Fig. 6, the suspension of silica particles is shown at different angles of the reactor tube. The oscillation conditions presented correspond to the minimum necessary oscillation amplitude at 12.1 Hz, to keep all the particles suspended. Silica particles were used since they are easier to observe due to the higher averaged particle diameter.

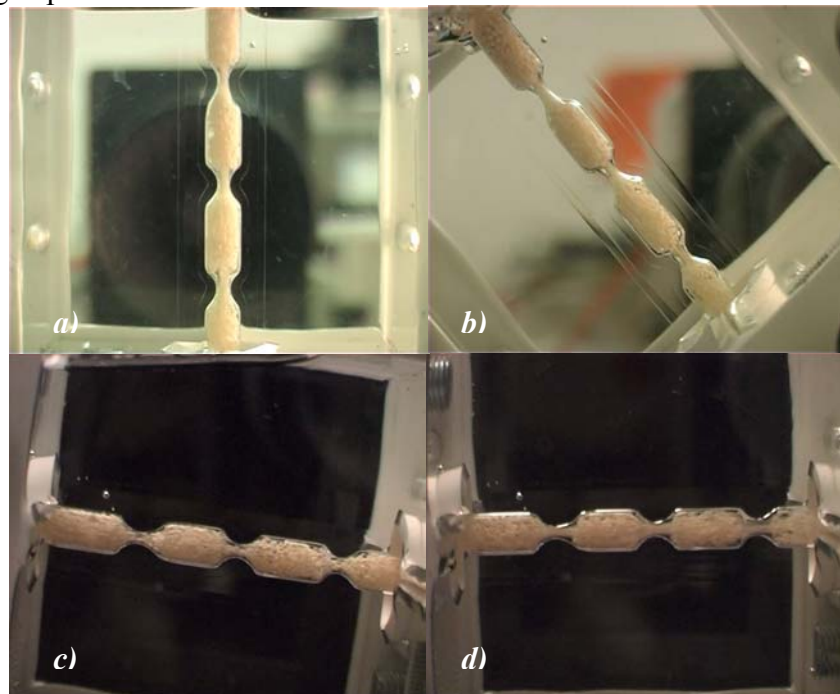


Fig.6 Suspension of 40 % (v/v) of silica particles at different angles and similar oscillation conditions: (a) vertical position,  $f = 12.1$  Hz,  $x_0 = 4$  mm; (b)  $45^\circ$ ,  $f = 12.1$  Hz,  $x_0 = 4$  mm; (c)  $10^\circ$ ,  $f = 12.1$  Hz,  $x_0 = 3$  mm; (d) horizontal position,  $f = 12.1$  Hz,  $x_0 = 3$  mm. In b), c) and d), right hand side correspond to the bottom of the tube and the left hand side corresponds to the top of the tube.



It was observed that it is easier to keep particles suspended in the horizontal than in the vertical position. For example, at 12.1 Hz, 3 mm of amplitude it is enough to keep 40 % (v/v) of silica resin particles completely suspended with the tube positioned horizontally but oscillation amplitude of 4 mm is needed to keep the same quantity of particles completely suspended when the tube is hold vertically.

Since in continuous operation some gas bubbles inlet through the input stream is frequent, the problem of gas washout should be considered during reactor design due to the micro scale of the SPC geometry. Therefore, the effect of the reactor angle on bubbles washout was also investigated, at the previously cited optimal oscillation conditions. The observations are not presented in this text but an auto-cleaning capacity of the micro-OFR was observed at angles above 45°. At low angles (near horizontal position) the small bubbles are retained inside each cavity. Furthermore, the presence of particles coupled with intensive mixing brakes the bubbles, aggravating this problem. Consequently, the washout of small bubbles controls the design angle.

The optimal angle for design of the novel micro-OFR was found to be 10°. At this position, all the bubbles can be cleaned from the system if a net flow of 14 mL.min<sup>-1</sup> (corresponding to a residence time of 20 s) is coupled with oscillatory flow with a specific periodicity. The cleaning time is less then 1 minute, for one tube operation.

A significant increase of the mean residence time of the bubbles was also observed when the fluid is oscillated at the optimal oscillations, even when the tube is positioned vertically. This capacity will be subject of study in the future.

Additional PIV measurements showed that the suspended particles follow the fluid and, consequently, the particles suspension parameters are related to the fluid mechanics. In Fig. 7, some results are presented from PIV measurement in the presence of silica resin particles (Fig. 7a) and polyamine particles (Fig. 7b).

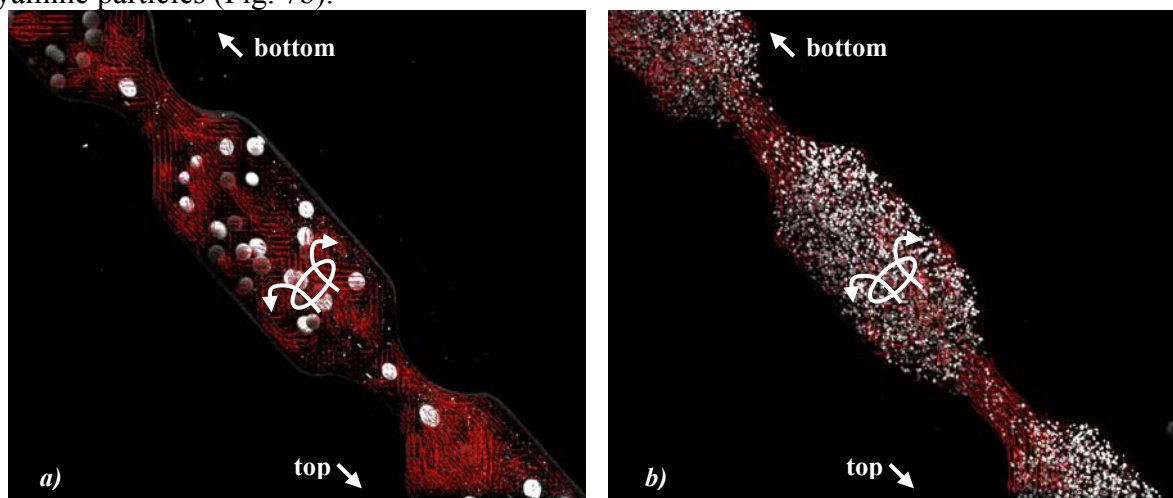


Fig.7 Flow patterns at oscillation conditions of  $f = 12.1$  Hz and  $x_0 = 3$  mm, at 45° of tube inclination: (a) velocity vector map of the tracer particles (fluid flow) in the presence of a small amount of silica particles (white elements in the picture); (b) velocity vector map of polyamine resin particles.

### 3.4 Micro reactor prototype

Once the capacity of the new micro-OFR for fluid mixing and particle suspension was proved, the design of the new micro reactor can be finally presented (Fig. 8). The idea is to couple a particular quantity of SPC tubes (this number can reach 30) and connected them in series, via a specific element able to fit a mesh on the top and bottom of each tube. Each tube can support different particles at different reaction temperatures. All the system is oscillated by a single unit, connected to the bottom of the first tube. It is also possible to have an input/output in each connection point to make the operation with sequential reactions possible.

A few units as the one presented in Fig.8 can be placed side-by-side to achieve a “multi micro-OFR” unit, which is a compact arrangement, able to carry on lots of different catalyst reactions in the same volume unit.

#### 4. Conclusions

This text has presented, for the first time, a novel micro scaled reactor based on the oscillatory flow technology (micro-OFR). This reactor is made by series of 30 cm long tubes, based on a new geometry, the smooth periodic cavity (SPC). It was demonstrated that it is possible to keep a high concentration of polymer bead-supported catalysts suspended in the micro-OFR and also to guarantee good fluid mixing. It has

also been shown that it is possible to prevent the retention of gas bubbles by configuring the tubes at an appropriate angle of 10°.

The new SPC geometry showed to be more suitable to micro-mixing and particle suspension applications than the conventional OFR geometry. Optimal oscillation conditions are  $f = 12.1$  Hz and  $x_0 = 3$  mm centre-to-peak.

Potential application areas for this novel reactor are specialty chemicals manufacture and high-throughput screening.

Future includes testing the performance of the micro-OFR as a continuous flow combinatorial, catalytic (homogeneous or heterogeneous) reactor. Further experiments concerning reaction engineering should be carried out, namely the hydrodynamic characterisation of the micro-OFR by means of residence time distributions (RTD's). Mass transfer and adsorption rates should also be determined in order to quantify the effect of fluid mechanics over fluid mixing and reaction rates.

#### 5. References

- Brunold, C. R., Hunns, J. C. B., Mackley, M. R. and Thompson, J. W., “Experimental Observations on Flow Patterns and Energy Losses for Oscillatory Flow in Ducts Containing Sharp Edges”, *Chem. Eng. Sci.*, 44, 1227 (1989).
- Dickens, A. W., Mackley, M. R. and Williams, H. R., “Experimental Residence Time Distribution Measurements for Unsteady Flow in Baffled Tubes”, *Chem. Eng. Sci.*, 44, 1471 (1989).
- Elgobashi, S., “On prediction particle-laden turbulent flows”, *Applied Science Research*, 52, 309-329 (1994).
- Fluent 5.5 users guide (1998), Vol. 1-4.
- Gao, S., X., Ni., Cumming, R. H., Greated, C. A. and Norman, P. I., “Experimental Investigation of Particle Flocculation in a Batch Oscillatory Baffled Reactor”, *Sep. Sci. Tech.*, 22, 2143, (1998).
- Howes, T. and Mackley, M. R., “Experimental Axial Dispersion for Oscillatory Flow Through A Baffled Tube”, *Chem. Eng. Sci.*, 45, 1349, (1990).
- Howes, T., Mackley, M.R. and Roberts, P.L., “The simulation of chaotic mixing and dispersion for periodic flows in baffled channels”, *Chem. Eng. Sci.*, 46, 1669-1677, (1991).

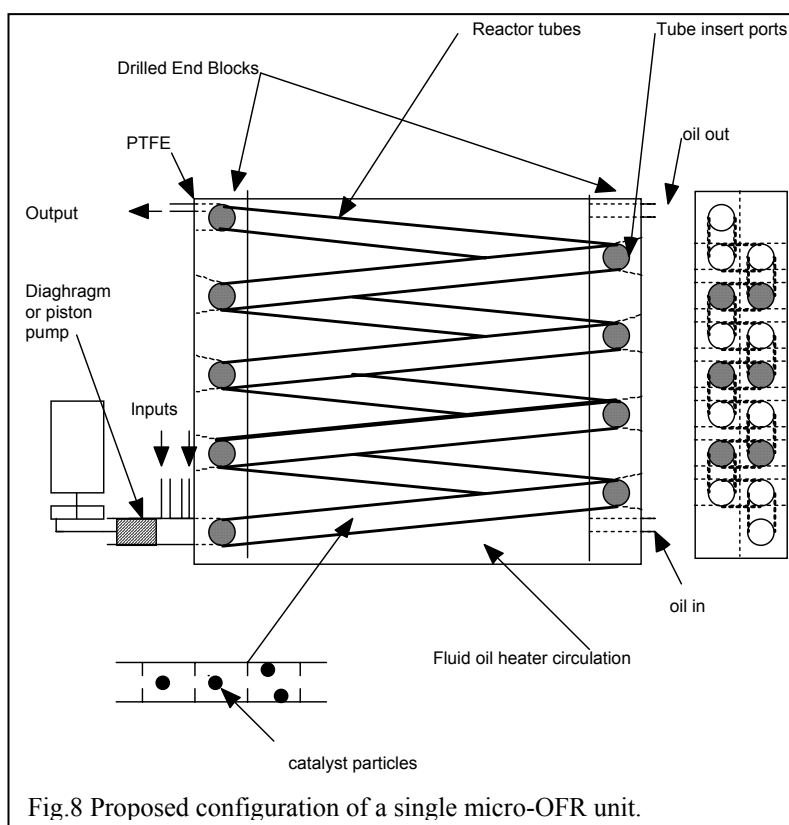


Fig.8 Proposed configuration of a single micro-OFR unit.

- Mackley, M.R., "Experimental heat transfer measurements for pulsative flow in baffled tubes", *Chem. Eng. Sci.*, 45, 1237-1242 (1990).
- Mackley, M.R., "Process innovation using oscillatory flow within baffled tubes", *Chem. Eng. Research & Design*, 74 (A5), 541-545 (1991).
- Mackley, M. R. and Ni, X., "Mixing and Dispersion in a Baffled Tube for Steady Laminar and Pulsative Flow", *Chem. Eng. Sci.*, 46, 3139 (1991).
- Mackley, M. R. and Ni, X., "Experimental Fluid Dispersion Measurements in Periodic Baffled Tube Arrays", *Chem. Eng. Sci.*, 48, 3293 (1993).
- Mackley, M.R., Smith, K. B. and Wise, N. P., "The Mixing and Separation of Particle Suspensions using Oscillatory Flow in Baffled Tubes", *Trans. Inst. Chem. Eng.*, 71, 649 (1993).
- Ni, X. and Gough, P., "On the discussion of the dimensionless groups governing oscillatory flow in a baffled tube", *Chem. Eng. Sci.*, 52(18), 3209-3212 (1997).
- Ni, X. and Pereira, N. E., "Parameter Affecting Fluid Dispersion in a Continuous Oscillatory Baffled Tube", *AIChE Journal*, 46, 37-45 (2000).
- Ni, X., Gao, S. and Pritchard, D. W., "A study of Mass Transfer in Yeast in a Pulsed Baffled Bioreactor", *Biotechnol. Bioeng.*, 45, 165 (1995a).
- Ni, X., Gao, S., Cumming, R. H. and Pritchard, D. W., "A comparative Study of mass Transfer in Yeast for a batch pulsed baffled bioreactor and a stirred tank fermenter", *Chem. Eng. Sci.*, 50(13), 2127-2136 (1995b).
- Ni, X., Zhang, Y. and Mustafa, I., "Correction of Polymer Particle Size with Droplet Size in Suspension Polymerisation of Methylmethacrylate in a Batch Oscillatory Baffled Reactor", *Chem. Eng. Sci.*, 54, 841, (1999).
- Ni, X., Cosgrove, J. A., Arnott, A.D., Greated, C.A. and Cumming, R.H., "On the measurement of strain rate in an oscillatory baffled column using particle image velocimetry", *Chem. Eng. Sci.*, 55, 3195-3208 (2000).
- Ni, X., Jian, H. and Fitch, A. W., "Computational Fluid Dynamic Modelling of Flow Patterns in an Oscillatory Baffled Column", *Chem. Eng. Sci.*, 57, 2849-2862 (2002).
- Stonestreet, P. and Harvey, A. P., "A mixing-based design methodology for continuous oscillatory flow reactors", *Trans. Inst. Chem. Eng.*, 80, Part A, 31-44 (2002).